Neutrosophic Fuzzy Logic based SVM approach for Enhanced Skin Cancer Prediction

Khaled Bedair [1], Ahmed H. Samak [2 *], Kottakkaran Sooppy Nisar [3], Ali Elrashidi [4], Amina Toumi [5], Shawkat Alkhazaleh [6], Afrah S. Albalawi [7], Rasha M. Abd El-Aziz [7,8]

[1]Sociology Program, Department of Social Sciences, College of Arts and Sciences, Qatar University, P.O. Box 2713, Doha, Qatar.

[2]Department of Computer Science, College of Computing and Information Technology, University of Bisha, Bisha 61922, Saudi Arabia.

[3]Department of Mathematics, College of Science and Humanities in Alkharj, Prince Sattam Bin Abdulaziz University, Alkharj 11942, Saudi Arabia.

[4]Department of Electrical Engineering, College of Engineering, University of Business and Technology, Jeddah, 21448, Saudi Arabia.

[5]Health Information Management Department, Liwa College of Technology, Abu Dhabi, United Arab Emirates.

[6]Department of Mathematics, Faculty of Sciences and Information Technology, Jadara University, Irbid, Jordan.

[7]Department of Computer Science, College of Science and Arts in Gurayat, Jouf University, Saudi Arabia.

[8]Information System Department, Faculty of Computers and Information, Assiut University, Assiut, Egypt.

Emails: khaledfb@qu.edu.qa, nhamed@ub.edu.sa, n.sooppy@psau.edu.sa, a.elrashidi@ubt.edu.sa, at_toumi@yahoo.fr, s.alkhazaleh@jadara.edu.jo, asblwiy@ju.edu.sa, rmhassanien@ju.edu.sa

Abstract

In this study, a thorough methodology is used to present a unique way for improving skin cancer prediction accuracy. The research uses sophisticated preprocessing methods, such as the Frost filter for noise reduction and histogram equalization for contrast enhancement, to boost contrast on dermoscopic pictures from various sources, using an ISIC 2020 dataset. These actions greatly raise the dermoscopic pictures' overall quality and usefulness for diagnosis. Utilizing labeled data for training, we offer a Fuzzy-based C-means clustering technique based on Neutrosophic Logic during the segmentation phase. In order to overcome ambiguities in skin lesion segmentation, the neutrosophic set—a groundbreaking idea in philosophy—is used. The suggested model enhances the accuracy of segmentation by modifying the neutrosophic set functions. For precise prediction, the approach combines Support Vector Machine (SVM) classification with Histogram of Oriented Gradient (HOG) feature extraction. While SVM, a supervised learning algorithm, diagnoses skin lesions based on the collected features, HOG features capture gradient information. To improve object recognition and classification, the HOG-SVM architecture is made to methodically collect and quantify essential information using dermoscopic pictures. The use of Neutrosophic Fuzzy Logic, which combines the benefits of fuzzy clustering with neutrosophic sets to produce more precise and nuanced predictions, sets the suggested method apart. The integration of different approaches into a holistic solution for skin cancer prediction is what makes the proposed study innovative. Findings and performance analysis show of the HOG-SVM method exhibits an outstanding accuracy of 98.69%, outperforming LR, KNN, and GNB methods. Python software is used to accomplish the suggested approach. This discovery opens up a possible path for better skin cancer diagnosis and advances the rapidly developing fields of dermatology and medical image processing.

Keywords: Skin Cancer Diagnostics; Neutrosophic Logic; Histogram of Oriented Gradient; Support Vector Machine; Frost Filter

DOI: https://doi.org/10.54216/IJNS.230226

Received: October 24, 2023 Revised: November 30, 2023 Accepted: December 29, 2023

1 Introduction

Skin cancer prediction is of paramount importance in the field of healthcare, considering the increasing prevalence of this potentially life-threatening condition.[1] Early intervention can be facilitated by accurate and timely prediction, which can improve treatment results and increase patient survival rates. Melanoma, squamous cell carcinoma, and basal cell carcinoma are the three primary kinds of skin cancer, which is a type of malignancy that starts in the skin cells.[2] The most dangerous kind, melanoma, originates from the melanocytes that produce pigment. Because of its increased propensity to spread, early identification is essential. While basal cell carcinoma originates in the basal cells, which are in charge of skin regeneration, squamous cell carcinoma grows in the squamous cells, which make up the skin's outer layer. Every kind has unique traits, thus correctly classifying them is necessary to develop effective treatment plans.[3] Utilizing cutting-edge technology like image analysis and machine learning can greatly aid in the creation of prediction models that can be used to diagnose skin cancer patients early and provide them with individualized therapy.[4]

Deep learning's use into skin lesion identification has transformed dermatology by providing a strong, automated method for identifying possible skin cancer indications. Convolutional neural networks (CNNs), in particular, are deep learning algorithms that have demonstrated extraordinary effectiveness in image classification tasks.[5] This makes CNNs a good fit for analyzing medical pictures, including skin lesions. These methods enable precise and effective identification of worrisome lesions by learning intricate patterns and characteristics from big datasets.[6] The capacity of deep learning to analyses several visual properties, including color, texture, and form, to find patterns indicative of benign or malignant lesions, is one of the major advantages of deep learning in skin lesion identification. Furthermore, when deep learning models are exposed to additional data, they may perform better and better over time, which leads to constant improvements in accuracy. Nevertheless, the use of deep learning to skin lesion detection has some restrictions, just like any other technique.[7] The requirement for extensive and varied datasets for training is one major obstacle. The quality and representativeness of the training data greatly influences the efficacy of deep learning models. Inadequate or prejudiced datasets can cause predictions to be off, making it more difficult to apply the model to a variety of patient groups.[8] Another issue is interpretability, as deep learning models sometimes act as "black boxes," making it challenging for medical experts to comprehend how the algorithm determines a certain diagnosis. The confidence and acceptance of these models in clinical practice may be hampered by their lack of openness.[9] Moreover, differences in imaging parameters like illumination, resolution, and camera quality might have an impact on how well deep learning models function in practical situations. For these models to be used in a variety of therapeutic settings, they must be robust to various environmental conditions.

It has shown to be quite successful to include machine learning into the prediction of skin cancer, providing a number of advantages that lead to faster and more precise diagnosis. The capacity of machine learning algorithms to examine enormous volumes of data, such as clinical photos, genetic data, and patient histories, in order to spot minute patterns and indicators linked to skin cancer, is one of its main benefits.[10] This data-driven method improves forecast accuracy and helps medical practitioners make well-informed choices. Machine learning models are quite good at extracting features and identifying patterns from complicated datasets, like dermatological pictures. This is especially true for models built on deep learning architectures. This capacity makes it possible to identify early indicators of skin cancer that may go undetected to the naked eye. In order to effectively manage skin cancer, early identification is essential since it allows for timely intervention and treatment, which can greatly improve patient outcomes.[11] Furthermore, machine learning models may be taught to learn and adapt on-the-fly, enhancing their prediction capabilities over time. This flexibility is especially useful when it comes to skin cancer, since fresh information and discoveries can be quickly added to the models to keep them abreast of the most recent developments in the area. Even though it's clear that machine learning is useful in predicting skin cancer, it's crucial to recognize that there are still issues to be resolved, including interpretability issues, data quality issues, and ethical issues. The benefits of using machine learning to forecast skin cancer are anticipated to increase when these problems are resolved, providing patients with better overall results and enhanced diagnostic capabilities.

A mathematical framework known as neutrosophic logic expands fuzzy and classical logic to deal with ambiguous, imprecise, and incomplete data. Although it has been used in a variety of fields, including as image processing and decision-making, its potential for use in the diagnosis of skin cancer is intriguing and should be investigated. Neuroscientific reasoning can be applied in the context of skin cancer prediction to address uncertainty related to diagnostic and medical data. The diagnosis of skin cancer is typically based on subjective evaluations, and different medical imaging may have different quality levels, making a precise categorization

DOI: https://doi.org/10.54216/IJNS.230226

Received: October 24, 2023 Revised: November 30, 2023 Accepted: December 29, 2023

difficult. Neutrosophic logic offers a more thorough and sophisticated framework for expressing uncertainty by allowing the representation of truth, indeterminacy, and falsehood. The interpretation of dermatological pictures is one possible use for neutrosophic logic in predicting skin cancer. Neutrophic sets are a useful tool for expressing the degree of integrity, uncertainty, and untruth related to the features taken from the pictures. Reflecting on the ambiguity involved in the interpretation of complicated visual patterns in skin lesions can improve the diagnosis process. Neutrosophic logic may also be included in machine learning algorithms that are used to forecast skin cancer. This makes it possible for the models to specifically address uncertainty throughout the learning process, leading to systems that are more resilient and flexible. These algorithms' decision-making processes may be enhanced using neutrophilic sets, offering a more versatile and sophisticated method of classifying skin cancers. Careful consideration should be given to developing efficient algorithms that can handle neutrosophic information and guarantee compatibility with current medical practices in order to address the challenges associated with the application of neutrosophic logic in skin cancer prediction as reported in the literature.

2 Related Work

Singh, Abolghasemi, and Anisi[12] offers the paper which proposes an improved deep learning algorithm to be used in conjunction with fuzzy logic-based picture segmentation for the diagnosis of skin cancer. This paper's use of pre-processing techniques, mathematical logic, average variance methodologies, and proposed L-R fuzzy de-fuzzification approach to improve segmentation outcomes is its standout feature. These pre-processing procedures are designed to eliminate artifacts like hair follicles and dermoscopic scales, among other things, in order to increase the visibility of lesions. The picture is then improved using the histogram equalization approach, and before the detection phase is carried out, it is segmented using the suggested method. The You Look Only Once neural network training technique is used in the upgraded model. This method was created by employing digital combined dermoscopic lesion images to identify melanoma lesions using DCNN. The YOLO method is made up of many DCNN layers to which researchers have added residual connections and a convolutional layer for additional depth. Additionally, researchers have combined multi-scale features at distinct levels by using feature concatenation. The results of the findings verify that YOLO outperforms the majority of the previous classifiers in relations of speed and accuracy score. The ISIC 2017 and the ISIC 2018 data sets' 2000 and 8695 dermoscopic pictures are used to train the classifier, while the PH2 datasets and the two previously stated datasets are utilized to test the suggested method.

Jaradat et al.[13] describes the study that found and assessed the best model for mpox detection using deep learning methods and classification models. To do this, this study examined the mpox identification accuracy scores of five widely used cellular deep learning models. The models' performance was evaluated through the use of metrics, specifically the accuracy, recall, precision, and F1-score. The results of our tests demonstrate that the model achieved an accuracy level of 98.16%, with a recall of 0.96, precision of 0.99, and an F1-score of 0.98, the MobileNetV2 model outperformed the others in terms of classification. Furthermore, employing the MobileNetV2 model produced the best accuracy of 0.94% when the model was validated using various datasets. The findings obtained in this paper show that for mpox picture classification, the MobileNetV2 approach performs better than earlier models that have been documented in the literature. These findings are encouraging since they demonstrate the potential application of machine learning methods for mpox early identification. this system demonstrated a high degree of accuracy in categorizing mpox, suggesting that it might be a useful tool for prompt and precise diagnosis in medical contexts.

A. Ogudo, Surendran, and Ibrahim Khalaf[14] offers an automated method for detecting and classifying skin lesions that combines a back propagation neural network using a feature extractor for an optimized stack sparse auto-encoder. This method is known as the OSSAE-BPNN methodology. A multilevel segmented approach is included in the suggested technique to identify the afflicted lesion location. Furthermore, for the identification of skin lesions, the BPNN-based classifier and the OSSAE-based feature extraction tool are utilized. Furthermore, the seagull optimization technique is used to tune the parameters of the SSAE model. In order to demonstrate the improved results of the (OSSAE-BPNN) approach, an extensive experimental study is conducted on the benchmark data. This papers result showed that, in terms of many assessment measures, the OSSAE-BPNN technique performed better than other existing strategies.

Gouda et al.[15] explains how to use the ISIC2018 dataset and a convolution neural network, which is a method of deep learning, to identify benign and malignant tumors. 3533 lesions of the skin total, comprising no

DOI: https://doi.org/10.54216/IJNS.230226

Received: October 24, 2023 Revised: November 30, 2023 Accepted: December 29, 2023

melanocytic, melanocytic, and malignant tumors, are included in the collection of data used in this investigation. Originally, the photos were enhanced and altered using ESRGAN. Preprocessing included resizing, normalizing, and enhancing the pictures. A CNN method may be used to categories images of skin lesions based on the final result attained after multiple iterations. Many learning transfer models were then used for fine-tuning, including Resnet50, InceptionV3, and Inception Resnet. What distinguishes and adds value to this study is the additional preprocessing step of using ESRGAN in addition to testing with other models. Results from the developed model were in line with those from the pre-trained models. Simulations conducted with the ISIC (2018) lesions of the skin dataset demonstrated the effectiveness of the proposed approach. While the accuracy rates of the Resnet50, InceptionV3, as well as Inception Resnet models, were 83.7%, 85.8%, & 84%, respectively, the CNN's accuracy rate was 83.2%.

Afza et al.[16] Proposes a innovative approach for multiclass skin tumor categorization utilizing a machine learning system and the best deep neural network feature fusion. This paper consists of five main steps: acquiring the image and enhancing its contrast; extracting deep learning features through transfer learning; selecting the best features through hybrid whale optimization plus entropy-mutual data method; fusing the chosen features through an improved canonical correlation-based method; as well as lastly, classifying the results using extreme learning machine based categorization. In this paper the two publicly accessible datasets, HAM10000 and ISIC2018, are used in the experiment. In this study both datasets, an accuracy of 93.40 & 94.36 percent was attained. The accuracy of this approach is higher than that of SOTA approaches. Moreover, the suggested approach exhibits computational efficiency.

Nigar et al.[17] provides a deep learning method utilizing Explainable Artificial Intelligence (XAI), which represents a major leap in the categorization of skin lesions. The difficulty of delayed detection owing to the high degree of resemblance across skin lesion categories in the initial phases of skin cancer is addressed in a well-articulated problem statement. While the report acknowledges the value of deep learning algorithms, it also acknowledges the inherent problem of mistrusting black box models, especially in medical settings where interpretability is critical. By offering justifications for model judgments, the suggested XAI-based skin lesion categorization method seeks to close this disparity and make dermatologists' interpretation and validation easier. With excellent accuracy, precision, recall, and F1 score for recognizing eight different kinds of skin lesions; the validation using the ISIC 2019 dataset shows encouraging findings. This guarantees the model's usability in actual clinical practice while also improving its accuracy. Overall, by fusing the interpretability of XAI with the capability of deep learning, this research greatly advances the field of skin cancer detection, meeting a crucial requirement for openness and confidence in medical AI applications.

Hatem[18] suggests using MATLAB to create an algorithm that can recognize skin lesions and categories them as benign or normal. Using the K-nearest neighbor (KNN) method, the classification procedure differentiates between benign skin lesions and those that are malignant, indicating disease. KNN is used because it is time efficient and promises highly accurate results. When classifying skin lesions, the system's classification accuracy reached 98%. Uncertain quantifying is crucial to optimization processes and influences the decision-making process in a big way. In image processing, computer vision, including medical image analysis, in particular, UQ is essential for ensemble machine learning methods and Bayesian approximations. To improve models, some research focuses on this particular idea. One example is a binary residual feature fusion model that uses Monte Carlo dropout and is used to classify medical images.

The presented literature encompasses diverse approaches to medical image analysis, particularly in the domain of lesion detection and segmentation. By combining fuzzy logic-based segmentation with an upgraded deep learning algorithm, the study suggests a better skin cancer prediction model. The model exhibits superior speed and accuracy with the use of L-R fuzzy de-fuzzification, YOLO deep neural network, and pre-processing techniques. It is successful in recognizing melanoma lesions using digital and dermoscopic pictures from the ISIC and PH2 datasets. Another approach combines deep learning algorithms with fuzzy logic-based segmentation for skin cancer diagnosis, utilizing pre-processing techniques, mathematical logic, and the YOLO deep neural network for improved results. A separate study focuses on the classification of mpox using various deep learning models, with MobileNetV2 demonstrating superior performance. Additionally, an automated method for skin lesion detection integrates a back propagation neural network with an optimized stacked sparse autoencoder, showcasing improved results compared to existing strategies. A convolutional neural network is utilized in another work for the detection of benign and malignant tumors in skin lesions, incorporating ESRGAN for image enhancement and achieving competitive accuracy rates. Finally, a novel approach for multiclass skin tumor categorization combines machine learning and deep neural network feature fusion, showcasing high

DOI: https://doi.org/10.54216/IJNS.230226

Received: October 24, 2023 Revised: November 30, 2023 Accepted: December 29, 2023

accuracy and computational efficiency. These diverse methodologies contribute to the ongoing efforts in developing precise and efficient medical image analysis techniques.

3 Problem Statement

The existing literature presents various innovative approaches to medical image analysis for skin cancer detection and classification. However, with the advancements, a thorough and improved prediction model that overcomes the shortcomings of existing techniques is still required. The literature identifies difficulties in managing ambiguity, optimizing classification results, and obtaining high accuracy in lesion segmentation. This work suggests a Neutrosophic Fuzzy Logic-based Support Vector Machine technique for improved skin cancer prediction to overcome these problems. The goal is to create a strong model that can manage ambiguity in medical pictures, increase the accuracy of lesion segmentation, and improve overall prediction performance for skin cancer detection by using the benefits of fuzzy logic, SVM, and Neutrosophic sets. In the context of skin cancer diagnosis, our research aims to improve upon the strengths of current approaches and develop precise and effective medical image analysis.[19]

4 Proposed Neutrosophic Fuzzy Logic based SVM for Skin Cancer Diagnosis

The proposed methodology employs a comprehensive approach for skin cancer prediction using dermoscopic images as shown in Fig 1. The dataset comprises 33,126 dermoscopic training pictures with distinct benign and malignant skin lesions from over 2,000 individuals, sourced from reputable institutions. The preprocessing technique involves applying the Frost filter for signal de-noising, enhancing image quality for diagnostic utility. Contrast enhancement through histogram equalization is employed to extract valuable features. Neutrosophic logic and a fuzzy-based C-means clustering algorithm are utilized for segmentation, distinguishing afflicted skin areas from healthy skin. The neutrosophic set introduces a nuanced approach to handling uncertainty in segmentation, enhancing accuracy. The methodology incorporates a HOG-SVM-based feature extraction and classification process, where Histograms of Oriented Gradients (HOG) capture gradient information for SVM-based classification. The overall approach demonstrates a systematic integration of preprocessing, segmentation, and classification techniques, leveraging advanced image processing and machine learning methods for accurate skin cancer prediction. The Frost filter, histogram equalization, neutrosophic logic, and HOG-SVM collectively contribute to a robust and effective framework for dermatological image analysis. The methodology is substantiated by results and discussions, showcasing its potential in advancing skin cancer diagnosis.

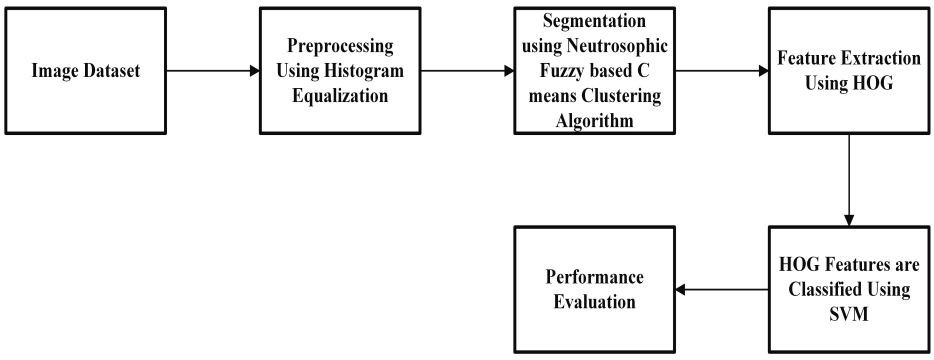

Figure 1: Proposed Framework for Skin Cancer Prediction.

4.1 Data collection

The collection consists of 33,126 dermoscopic training images of unique benign and malignant skin lesions from over 2,000 individuals. All of these individuals are associated with each image through a unique patient

DOI: https://doi.org/10.54216/IJNS.230226

Received: October 24, 2023 Revised: November 30, 2023 Accepted: December 29, 2023

ID. While expert opinion, longitudinal follow-up, or histology has been used to confirm benign diagnoses, histology has been utilized to confirm all malignant diagnoses. The International Skin Imaging Collaboration (ISIC) created the dataset with images from the following source institutions: Hospital Clínic de Barcelona, Medical University of Vienna, Memorial Sloan Kettering Cancer Centre, Melanoma Institute Australia, University of Queensland, and University of Athens Medical School.[20]

4.2 Preprocessing using Frost Filter

The study suggests a unique preprocessing technique that applies the Frost filter, a flexible adaptive filter well-known for its efficacy in signal de-noising, to improve the image quality of DERMOSCOPIC pictures. By calculating local statistics inside a noisy signal and using this knowledge to effectively filter out unwanted noise components, the Frost filters works on this basic idea. A methodical methodology is used to apply the Frost filter in the framework of DERMOSCOPIC picture enhancement.[21] First, the noisy image's statistics—that is, its mean and variance—are calculated. The noise power spectrum is then calculated, which is an important parameter for filter design. Next, using the predicted noise power spectrum and the local data, filter coefficients are calculated for every pixel. The noisy DERMOSCOPIC image is then subjected to the meticulously constructed Frost filter, producing an output that is refined and de-noised.[22] In medical applications, this preprocessing procedure has the probable to greatly improve the DERMOSCOPIC pictures' overall superiority and diagnostic utility. Equation of the frost filter is given in Eq. (1),

$$F_f = \sum_{n\times n} K\ \alpha e^{-\alpha|t|} \tag{1}$$

$$\alpha = \left(\frac{4}{n\sigma^{-2}}\right)\left(\frac{\sigma^2}{\overline{I}^2}\right) \tag{2}$$

Where, $|t| = |X - X_0| + |Y - Y_0|$. K Denotes normalized constant, $\overline{I}$ denotes local mean, σ denotes local variance, variation of image co-efficient is defined as $\overline{\sigma}$ where, moving kernel size is represented as n.

4.2.1 Contrast Enhancement Using Histogram Equalization

In the field of medical imaging, contrast enhancement is a crucial step in raising an image's local contrast. The contrast stretching technique is often used in medical image processing to accurately detect skin lesions; in this stage, however, it is being used to extract additional valuable features.[23]

$$\overline{c}\,[\rho] = \sum_{n=0}^{\rho} \overline{h}\,[x]\,,\ \rho = 0, 1, \ldots, 255 \tag{3}$$

The provided Equation (3) represents the calculation of the consecutively entirety of a histogram ($\overline{c}\ [\rho]$) based on the gray levels (ρ). The running sum is computed using the cumulative sum of the histogram values up to a specific gray level (ρ). where $\overline{h}$ represents the floating point value.

4.3 Neutrosophic Logic and Fuzzy based C- means Clustering Algorithm for Segmentation

The process of dividing the afflicted skin area from the healthy skin is known as segmentation. Use labeled data to train the neutrosophic set-based segmentation model, where the neutrosophic sets stand-in for ground truth annotations.[24] To improve segmentation accuracy, adjust the neutrosophic set functions' settings.

DOI: https://doi.org/10.54216/IJNS.230226

Received: October 24, 2023 Revised: November 30, 2023 Accepted: December 29, 2023

4.3.1 Neutrosophic image

NS is referred as the image set : let X = $\{X_1,\ X_2, \ldots..X_m\}$ as a set of alternatives in neutrosophic set. The alternative X_i is {T(X_i), I(X_i),F (X_i))}/ X_i , where T(X_i), I(X_i) and F(X_i) are the values corresponding to the true, false, and indefinite membership sets. Neutronosophic images, designated as M_i in NS, are image Ims that are interpreted using Ts, Is, and Fs. The interpretation of a given I_{NS} pixel P(a, b) is P_{NS}(a, b) = {Ts(a,b), Is(a,b), Fs(a,b)}. The memberships that belong to the background, indeterminate set, and foreground are represented by Ts(a,b), Is(a,b), and Fs(a,b), respectively. The true and indeterminacy memberships are utilised to characterise the indeterminacy within the local neighbourhood as follows, based on the intensity value and local geographical information:

$$Ts\,(a,b) = \frac{g\,(a,b) - g_{min}}{g_{max} - g_{min}} \tag{4}$$

$$I_s\,(a,b) = \frac{Gd_{(a,b)} - Gd_{min}}{Gd_{max} - Gd_{min}} \tag{5}$$

In Eqn (4) and (5) the intensity and gradient magnitude at the pixel of (a,b) on the image are represented by g(a,b) and Gd(a,b).

Additionally, research employ the global intensity distribution to compute the neutrosophic membership values, taking into account the indeterminacy of intensity across various groups. Neutrophic c-means clustering (NCM) solves the issues that other algorithms have with managing undetermined points. Here, research employ NCM to determine the unpredictability values on intensity to be segmented amongst various groups. The reality and indeterminacy memberships are specified using NCM as mentioned in Eqn (6):

$$K = \left[\frac{1}{\beta_1}\sum_{n=1}^{Z}(a_m - z_n)^{-\frac{2}{u-1}} + \frac{1}{\beta_2}(a_m - \overline{z}_{imax})^{-\frac{2}{u-1}} + \frac{1}{\beta_3}\gamma^{-\frac{2}{u-1}}\right]^{-1} \tag{6}$$

$$Tb_{mn} = \frac{K}{\beta_1}(a_m - z_n)^{-\frac{2}{u-1}} \tag{7}$$

$$Ib_m = \frac{K}{\beta_2}(a_m - \overline{z}_{imax})^{-\frac{2}{u-1}} \tag{8}$$

where $\overline{z}_{imax}$ is determined using the indices of the highest and second largest value of Tij.

4.3.2 Indeterminacy Filtering

In order to eliminate the impact of indeterminacy information for segmentation, a new filter is defined based on the indeterminacy, and the kernel function is defined using a Gaussian function as follows:

$$D_1\,(i,j) = \frac{1}{2\pi\sigma_i^2}\exp(\frac{i^2+j^2}{2\sigma_1^2}) \tag{9}$$

$$\sigma_1\ (a,b) = f\,(I\,(a,b)) = xI\,(a,b) + y \tag{10}$$

where is defined as a function f(·) connected to the indeterminacy degree, and σ_I is the standard deviation value. A high degree of indeterminacy results in a big σ_I, which can be filtered to smooth out the present local neighbourhood. A low indeterminacy level results in a small σ_I and less seamless filtering of the local neighbourhood. The Gaussian function should be used because it can more smoothly translate the undetermined degree to a filter weight.

T_s(a,b) is filtered indeterminately, which makes it more homogeneous.

$$T^{'}{}_s\,(a,b) = Ts\,(a,b)\bigoplus GI_s\,(i,j) = \sum_{j=b-m/2}^{b+m/2}\sum_{i=a-m/2}^{a+m/2} Ts(a-i,b-j)(i,j) \tag{11}$$

DOI: https://doi.org/10.54216/IJNS.230226

Received: October 24, 2023 Revised: November 30, 2023 Accepted: December 29, 2023

$$D_{Is}\left(i,j\right)=\frac{1}{2\pi\sigma_i^2}\exp(-\frac{i^2+j^2}{2\sigma_{Is}^2}) \tag{12}$$

$$\sigma_{Is}\ \left(a,b\right)=f\left(Is\left(a,b\right)\right)=xIs\left(a,b\right)+y \tag{13}$$

In Eqn (11) – (13) $T'_s$is the outcome of the indeterminate filtering. The linear function that converts the indeterminacy level to a parameter variable has two parameters: x and y.

After NCM, the filtering is likewise applied to $T_{nuv}(a,b)$. After indeterminacy filtering, the local spatial neutrosophic value serves as the NCM's input.

$$Tn^{'}{}_{uv}\left(a,b\right)=Tn_{uv}\left(a,b\right)\bigoplus D_{In}\left(i,j\right)=\sum_{j=b-m/2}^{b+m/2}\sum_{i=a-m/2}^{a+m/2}Tn_{u,v}(a-i,b-j)D_{In}(i,j) \tag{14}$$

$$D_{Is}\left(i,j\right)=\frac{1}{2\pi\sigma_{In}^2}\exp(-\frac{i^2+j^2}{2\sigma_{In}^2}) \tag{15}$$

$$\sigma_{In}\left(a,b\right)=f\left(In\left(a,b\right)\right)=zIn\left(a,b\right)+w \tag{16}$$

where m is the filter kernel size and Tn'_{uv} is the indeterminate filtering result on T_s. The image is segmented using a maximum-flow technique, and a graph is constructed usingTn'_{uv}.

4.3.3 Neutrosophic Graph Cut

A graph D = (D,E) is divided into two subsets, K and L, by a cut C = (K,L). The set $\{(i, j) \in E|u \in K, \vartheta \in T\}$ of edges with one endpoint in S and the other endpoint in T is the cut set of a cut C = (K,L). By defining in terms of energy reduction, which is converted into the maximum flow problem in a graph or a minimal cut of the graph, graph cuts can effectively address picture segmentation difficulties.

Typically, the energy function consists of two parts: smooth constrict $E_{smt}\ \rightarrow Esmoth$ and data constrict $E_{dt}\rightarrow Edata.$

$$E\left(f\right)=E_{dt}\left(f\right)+E_{smt}(f) \tag{17}$$

In Eqn (17) f denotes map that divides pixels into various categories. While E_{smt} assesses the degree to which f is piecewise smooth and may be shown as an n-link in a graph, E_{dt} examines the discrepancy between f and the designated region, which can be represented as a t-link. The energy function is implemented differently in different models. The Potts model-based function is described as follows

4.3.4 Neutrosophic set

A novel area of philosophy known as the neutrosophic set (NS) was proposed, addressing, character, in addition to their relationships with a wide range of other ideational spectrums. A neutrosophic set item, E, is examined in relation to its opponent, 'Anti-E,' and its neutrality, 'Neut-E,' which is neither 'E' nor 'Anti-E.' Additionally, the extent to which 'E' is true, ambiguous, or false is measured using three memberships. An excellent tool for dealing with uncertainty is the neural network (NS), which has produced practical applications in many different fields, including database management systems (DBMS), language online services, economic dataset identification, and new economic development and decline analysis.[25]

$\widetilde{\boldsymbol{A_{Nus}}}$ is termed as a neutrosophic set if $\widetilde{\boldsymbol{A_{Nus}}}=\left\{\left(\boldsymbol{x};\left[\boldsymbol{\alpha}_{\widetilde{\boldsymbol{A_{Nus}}}}\left(\boldsymbol{x}\right),\boldsymbol{\beta}_{\widetilde{\boldsymbol{A_{Nus}}}}\left(\boldsymbol{x}\right),\boldsymbol{\gamma}_{\widetilde{\boldsymbol{A_{Nus}}}}\right]\right)\ :\boldsymbol{x}\boldsymbol{\epsilon}\boldsymbol{X}\right\}$,

Where $\boldsymbol{\alpha}_{\widetilde{\boldsymbol{A_{Nus}}}}\left(\boldsymbol{x}\right)\ :\boldsymbol{X}\rightarrow]\boldsymbol{0}^{-},\boldsymbol{1}^{+}[$ is termed as the truth function, $\boldsymbol{\beta}_{\widetilde{\boldsymbol{A_{Nus}}}}\left(\boldsymbol{x}\right):\boldsymbol{X}\rightarrow[\boldsymbol{0}^{-},\boldsymbol{1}^{+}]$ is called the hesitant function, and$\boldsymbol{\gamma}_{\widetilde{\boldsymbol{A_{Nus}}}}\ \left(\boldsymbol{x}\right)$: $\boldsymbol{X}\rightarrow[\boldsymbol{0}^{-},\boldsymbol{1}^{+}]$ is called the falsity function. Additionally,$\boldsymbol{\alpha}_{\widetilde{\boldsymbol{A_{Nus}}}}\left(\boldsymbol{x}\right)$, $\boldsymbol{\beta}_{\widetilde{\boldsymbol{A_{Nus}}}}\left(\boldsymbol{x}\right)$ and $\boldsymbol{\gamma}_{\widetilde{\boldsymbol{A_{Nus}}}}\ \left(\boldsymbol{x}\right)$ satisfy the following the relation:

$$\boldsymbol{0}^{-}\leq\boldsymbol{sup}\left\{\boldsymbol{\alpha}_{\widetilde{\boldsymbol{A_{Nus}}}}\left(\boldsymbol{x}\right)\right\}+\boldsymbol{sup}\left\{\boldsymbol{\alpha}_{\widetilde{\boldsymbol{A_{Nus}}}}\left(\boldsymbol{x}\right)\right\}+\boldsymbol{sup}\left\{\boldsymbol{\alpha}_{\widetilde{\boldsymbol{A_{Nus}}}}\left(\boldsymbol{x}\right)\right\}\leq\boldsymbol{3}^{+} \tag{18}$$

DOI: https://doi.org/10.54216/IJNS.230226

Received: October 24, 2023 Revised: November 30, 2023 Accepted: December 29, 2023

The relationship between truth, reluctance, and falsity degrees is balanced, limiting extreme values and encouraging a more nuanced portrayal. With the existing cluster centres C in mind, update the neutrosophic membership values U.

$$Tij = \frac{1}{1 + \frac{d(x_i,\, c_j)}{\lambda}} \tag{19}$$

$$Iij = \frac{1}{1 + \frac{|d(x_i,\, c_j)|}{\lambda}} \tag{20}$$

$$Fij = \frac{1}{1 + \frac{d(x_i,\, c_j)}{\lambda}} \tag{21}$$

where λ is a parameter that regulates how much distance affects membership values. First, random initializations are made for the fuzziness parameter and the cluster centers. Next, until convergence, the centroids and membership degrees are modified frequently. To generate the segmentation result, each pixel is allocated to the cluster having its highest degree of membership. Initialization of a degree of membership metrics is followed by the determination of the cluster centroids and the updating of the degrees of membership metrics for each data point based on the separation between each cluster centroid with the data point. After the degree of membership numbers are updated, the cluster centres are calculated again using the average weighted of the data points. Keep going until you reach convergence. Once the process has converged, each data point is finally assigned to the cluster with the largest degree of membership value.

Let's assume that there are n finite datasets and that X = (x1, x2,. . . .,xn). The FCM technique is used to partition the dataset X into cluster groups. The FCM algorithm formula may be found in Equation (22).

$$J_s = \sum_{p=1}^{n} \sum_{q=1}^{c} u_{pq}^{s} \left\| X_p - C_q \right\|^2 \tag{22}$$

Where $c_q$is the q^{th} cluster centre, s indicates the fuzzy variable, and $\| \ \|$ is the distance measured using Euclid. Additionally, u_{pq} is the amount of membership value of k_p in the q^{th}clusters.

$$u_{pq} = \frac{1}{\sum_{k=1}^{c} \left(\frac{d_{pq}}{d_{kq}^{*}} \right)^{\frac{2}{s-1}}} \tag{23}$$

$$c_j = \frac{\sum_{q=1}^{n} u_{pq}^{s}}{\sum_{q=1}^{n} u_{pq}^{s}} k_p \tag{24}$$

Where, d_{pq} specifies the distance between the data point k_p and q^{th} cluster center and d_{kq}^{*} is the distance among k^{th} cluster center and q^{th} cluster centers.

4.4 HOG-SVM Based Feature Extraction and Classification

The HOG-SVM based feature extraction and classification method involve first extracting HOG features from the image, capturing its gradient information in a histogram representation. These features are then utilized as input for training an SVM classifier, which learns to discriminate between different classes based on the extracted features. In the classification phase, the trained SVM is employed to predict the class labels of new data points by evaluating their HOG features.[26]

A type of descriptor that finds object characteristics using computer vision & image processing technologies is the Histogram of Oriented Gradient feature. By computing a statistical histogram of the direction gradient in a particular region of the picture, features may be retrieved. In the realm of picture identification, the integration of the SVM classifier with Hog feature extraction has been widely used. A set of procedures is involved in the feature extraction process employing Histogram of Oriented Gradients (HOG) in order to identify and represent the salient aspects of a picture, especially when it comes to object recognition. Defining a detection

DOI: https://doi.org/10.54216/IJNS.230226

Received: October 24, 2023 Revised: November 30, 2023 Accepted: December 29, 2023

window is the initial phase, in which the picture is methodically split into many windows, blocks, and cells. Then, several cells are generated inside each block that is further separated into windows. These cells are the building blocks of feature extraction and stay still throughout the procedure.[27]

The next stage after window, block, & cell division is picture normalization. Gamma and color room normalization are used in this normalization process to minimize the effects of changing illumination and prevent disproportionate contributions from certain image regions. The intended outcome determines how the gamma value should be changed. The standard formula for gamma compression:

$$l(a,b) = l(a,b)^{\gamma} \tag{25}$$

γ accepts values according to the result. The calculation of gradients is what comes next. The gradient orientation is obtained from these estimated values, which are obtained by computing the gradients in both the horizontal and vertical orientations. Comprehending the directionality of the pixel intensity variations in the picture requires completing this step. The following is the formula:

$$Ga(a,b) = H(a+1,b) - H(a-1,b) \tag{26}$$

$$Gb(a,b) = H(a,b+1) - H(a,b-1) \tag{27}$$

The two formulae, $Ga(a,b)\ and\ Gb(a,b)$, respectively, represent the pixel value at a particular pixel location in the gathered image as well as the aclinic and perpendicular gradients. At pixel $(a,\ b)$, the gradient direction and gradient value are as follows:

$$G(a,b) = \sqrt{Ga(a,b)^2 + Gb(a,b)^2}\alpha(a,b) = tan^{-1}\left(\frac{Gb(a,b)}{Ga(a,b)}\right) \tag{28}$$

In order to create gradient column diagrams, the perspective of data is separated into bins, typically consisting of nine bins. An image's orientation information is discretized and represented by each bin, which relates to a range of gradient orientations. The cell-normalized gradient histogram is then computed for every block after that. In order to lessen the effects of foreground-background contrast and local light fluctuations on the gradient intensity, this normalization is crucial. Lastly, all of the normalized gradient histograms from every block are combined to create the HOG feature vectors. The unique spatial and orientation properties of the picture are well captured by this feature vector, which strengthens its representation for further tasks like object recognition.

The HOG feature extraction method methodically extracts and measures pertinent information from various parts of the picture, which make it useful for tasks like object detection and categorization as shown in Fig 2. In machine learning, the supervised learning model of the support vector machine and the associated learning method are commonly employed. It may be applied to regression analysis and data categorization. Each sample is labeled as one of two varieties when given a set of training specimens. The SVM drill method then builds an unpredictability binary linear classifier, sets up a model, and assigns the fresh specimens to a certain variety. The SVM training model splits the specimens with a clear and broad gap, representing all specimens as mappings of points in space. After that, the fresh specimens are categorized and mapped in the same room.

DOI: https://doi.org/10.54216/IJNS.230226

Received: October 24, 2023 Revised: November 30, 2023 Accepted: December 29, 2023

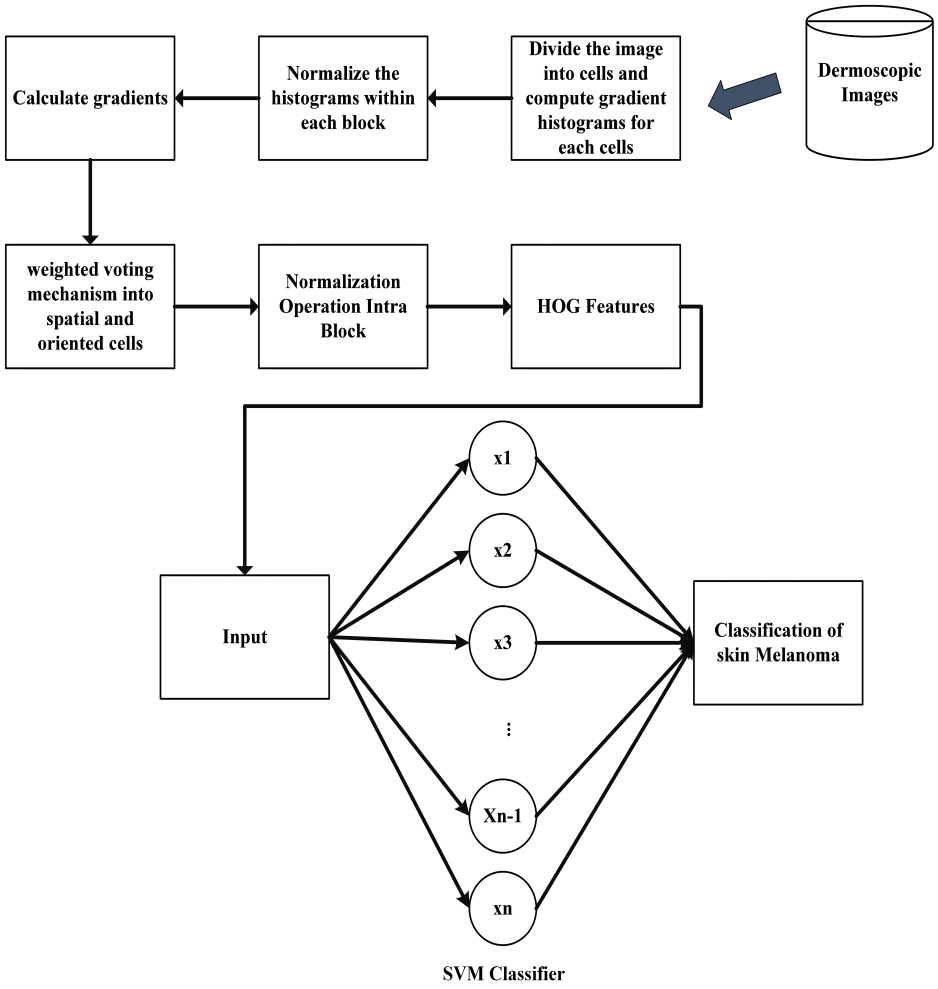

Figure 2: Proposed HOG-SVM Architecture for Skin Cancer Prediction.

Algorithm 1: HOG-SVM
Input: *Dermoscopic images from ISIC 2020 dataset*
Output: *classifying skin lesions*
Load input image data
$X=\{x_1,x_2,x_3,\ldots x_n\}$ *// data acquisition*
Pre-processing of images
Noise removal of Dermoscopic images //frost filter
Contrast Enhancement //Histogram Equalization
Segmentation of Preprocessed images //Neutrosophic and Fuzzy clustering
Initialize the no. of clusters and the membership values
Calculate the centroids of the cluster
Update the membership values
if (membership value is non-negative)
Updates iteratively until convergence is met
else
Convergence is not met
end if
Maximum number of iterations is reached
Feature extraction //HOG
Classification //SVM

DOI: https://doi.org/10.54216/IJNS.230226

Received: October 24, 2023 Revised: November 30, 2023 Accepted: December 29, 2023

5 Results and Discussion

A number of performance indicators are used in the results and discussion section to assess how well the suggested Neutrosophic Fuzzy Logic-based SVM technique for Enhanced Skin Cancer Prediction works. The four main metrics—accuracy, precision, recall, and F1-score—each offer a different perspective on the predictive power of the model. Recall analyses the model's capacity to accurately identify positive cases, accuracy gauges the overall correctness of predictions, precision gauges the accuracy of optimistic forecasts, and the F1-score balances accuracy and recall. Together, these measures provide a thorough evaluation of the model's diagnostic precision and efficacy in differentiating between benign and malignant skin lesions. The suggested methodology is deemed better and its possible consequences in dermatological image analysis and skin cancer prediction are thoroughly analyzed. The discussion places these metrics in the context of current methodologies and interprets them accordingly.

5.1 Dataset

Training Dataset For training purposes, the dataset is meticulously structured to facilitate the development and optimization of algorithms as shown in Fig 3. The dermoscopic images are paired with ground truth annotations, confirming the diagnoses through histology for malignant cases and utilizing expert opinion, longitudinal follow-up, or histology for benign cases. This annotated training set forms the basis for teaching the model to recognize and distinguish between different skin lesions accurately.

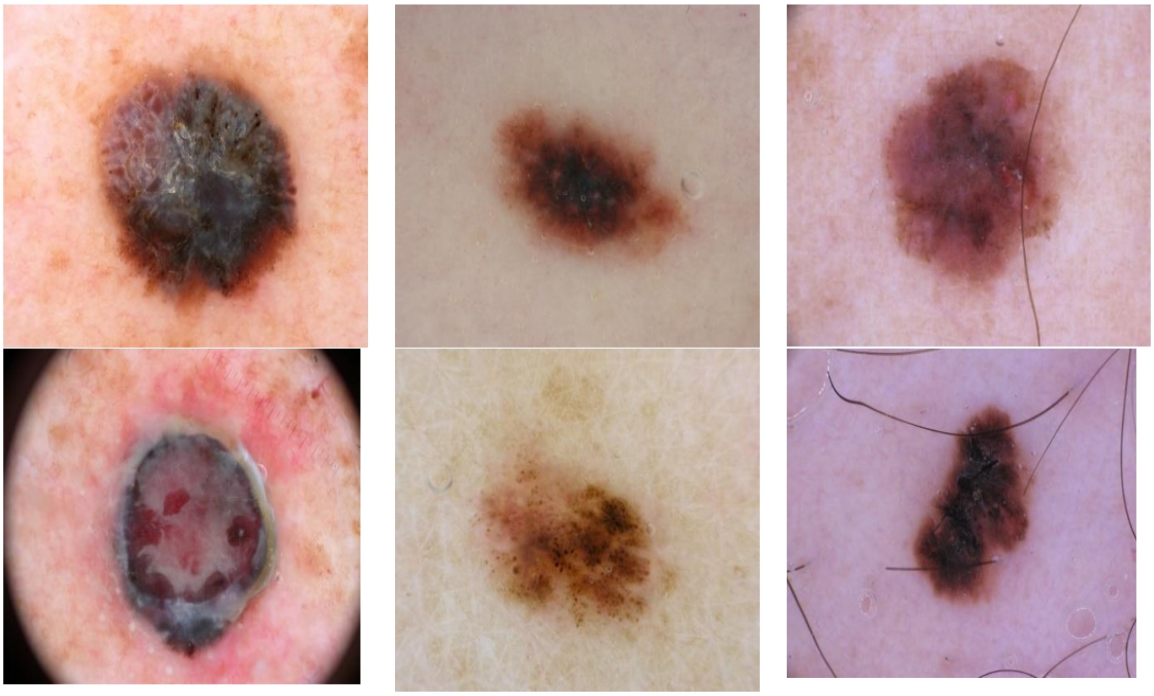

Figure 3: Example of Images Taken for Training from ISIC 2020 Databases to Classify Malignant vs. Benign Tumors.

Testing Dataset The testing set is designed to estimate the method's generalization and predictive capabilities on unseen data as shown in Fig 4. It comprises a separate subset of dermoscopic images, distinct from the training set, ensuring that the model's performance is assessed on novel and previously unseen cases. The testing set is also accompanied by ground truth annotations to objectively measure the model's accuracy, sensitivity, and specificity in identifying benign and malignant skin lesions. The meticulous curation of the training and testing sets within the ISIC 2020 dataset underscores the reliability and validity of the model's predictions, contributing to the robustness of the proposed Neutrosophic Fuzzy Logic-based SVM approach for enhanced skin cancer prediction.

DOI: https://doi.org/10.54216/IJNS.230226

Received: October 24, 2023 Revised: November 30, 2023 Accepted: December 29, 2023

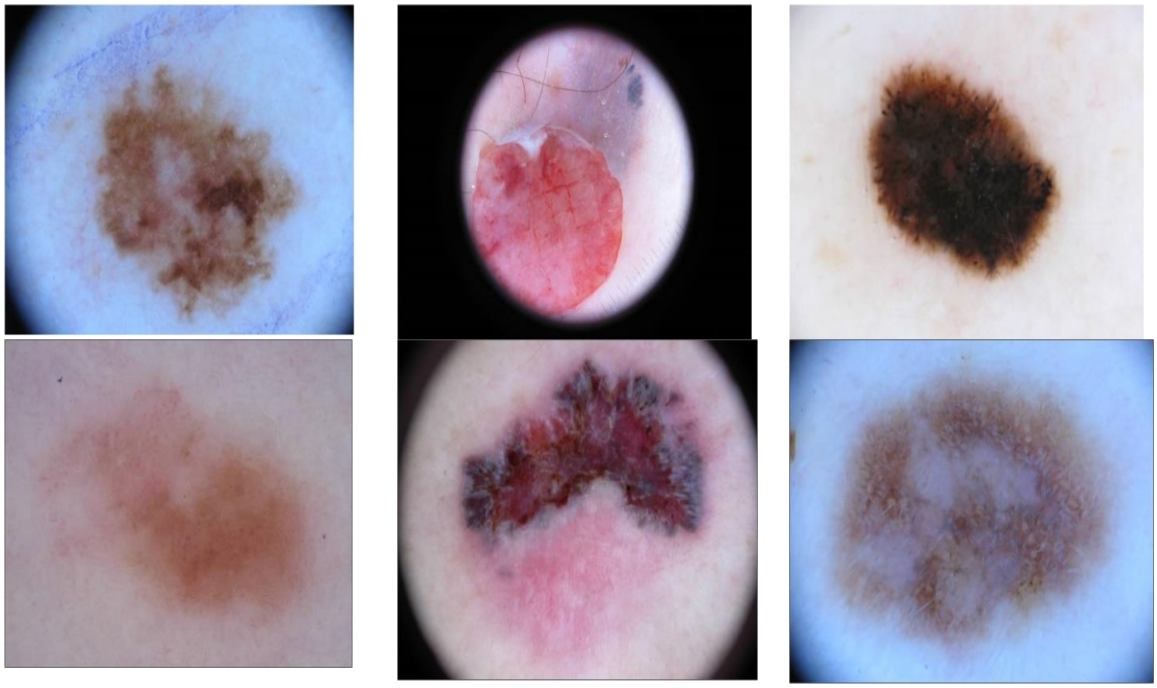

Figure 4: Example of Images Taken for Testing from ISIC 2020 Databases for Classification of Benign vs. Malignant Tumors.

5.2 Performance Evaluation

Accuracy

Accuracy is used to evaluate the proposed system's efficacy across all categories. It is the idea that each observation would be accurately anticipated in general. The precision is expressed in equation (29).

$$Accuracy = \frac{T_{Pos} + T_{Neg}}{T_{Pos} + T_{Neg} + F_{Pos} + F_{Neg}} \tag{29}$$

Precision

The precise positive evaluations that deviate from the overall positive evaluation are counted to determine precision. Equation (30) can be used to determine the precise diagnosis of pneumonia,

$$P = \frac{T_{Pos}}{T_{Pos} + F_{Pos}} \tag{30}$$

Recall

The ratio of all positive samples to real positives that were accurately classified as positives is known as recall. The percentage of correctly predicted cases of pneumonia identified by equation (31) is given.

$$R = \frac{T_{Pos}}{T_{Pos} + F_{Neg}} \tag{31}$$

F1-Score

Recall and accuracy are used to calculate the F1-Score. Equation (32) represents the F1-Score, which is calculated using precision and recall.

$$F1\text{-}score = \frac{2 \times precision \times recall}{precision + recall} \tag{32}$$

DOI: https://doi.org/10.54216/IJNS.230226

Received: October 24, 2023 Revised: November 30, 2023 Accepted: December 29, 2023

Table 1: Comparison of Proposed HOG-SVM with Existing Methods.

Methods	Accuracy (%)	Precision (%)	Recall (%)	F1-score (%)
LR, KNN, GNB[28]	93.0	92.34	92.65	93.2
CNN[29]	92	91.90	89.65	90.3
Deep Belief Network[29]	86.06	93.87	92.10	90.67
Proposed HOG-SVM	98.69	96.65	94.34	95.67

A comparison of skin cancer prediction techniques is shown in Table 1, which also includes performance indicators such as accuracy, precision, recall, and F1-score. According to Bechelli and Delhommelle's 2022 report, three methods—LR (Logistic Regression), KNN (K-Nearest Neighbours), and GNB (Gaussian Naive Bayes)—achieved an accuracy of 93.0%, with values for precision, recall, and F1-score ranging from 92.34% to 93.2%. An accuracy of 92% was shown using a Convolutional Neural Network, with values for precision, recall, and F1-score ranging from 91.90% to 90.3%. A Deep Belief Network was used in another technique that Tahir et al. (2023) reported that produced an accuracy of 86.06%, with precision, recall, and F1-score ranging from 93.87% to 90.67%. The suggested HOG-SVM technique, on the other hand, fared better than these methods, achieving a much higher accuracy of 98.69% in addition to improved precision, recall, and F1-score values, highlighting its usefulness in the prediction of skin cancer.

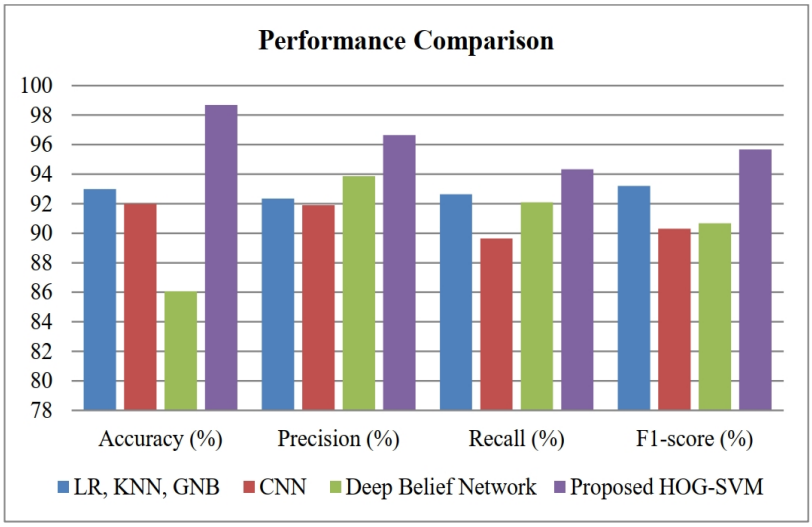

Figure 5: Comparison of Performance with Existing Methods.

Figure 5 visually represents these metrics, providing a comprehensive overview of the comparative performance of the various methods, with the proposed HOG-SVM method standing out as a highly accurate and precise approach for skin cancer prediction.

Table 2: Comparing the Performance of Existing Dataset with ISIC 2020 dataset.

Datasets	Accuracy (%)	Sensitivity (%)	Specificity (%)
ISIC 2017[12]	97.65	96.5	96.3
ISIC 2019[12]	94.7	96.4	94.3
ISIC 2020 (Proposed)	98.69	97.45	97.56

According to Singh, Abolghasemi, and Anisi's 2023 study, Table 2 displays metrics for accuracy, sensitivity, and specificity for three distinct datasets. The ISIC 2020 database performs better than the others in terms

DOI: https://doi.org/10.54216/IJNS.230226

Received: October 24, 2023 Revised: November 30, 2023 Accepted: December 29, 2023

of accuracy, with a whopping 98.69%, as opposed to 97.65% for ISIC 2017 and 94.7% for ISIC 2019. The capacity of the model to accurately detect affirmative cases is measured by sensitivity, which is highest for ISIC 2020 at 97.45%, closely followed by ISIC 2017 at 96.5% and ISIC 2019 at 96.4%. ISIC 2020 likewise has the greatest specificity (97.56%), which measures the model's accuracy in recognizing negative situations. ISIC 2017 (96.3%) and ISIC 2019 (94.3%) are the next best. The outcomes point to a significant improvement in the accuracy and specificity of the planned ISIC 2020 dataset, suggesting that it has the potential to be a reliable dataset for dermatological image analysis.

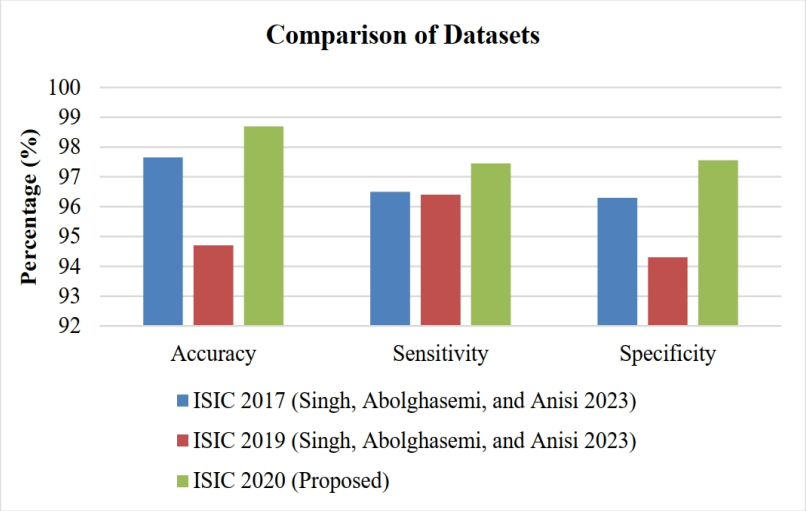

Figure 6: Comparison of Datasets.

The merits and disadvantages of these datasets for dermatological image classification tasks may become clearer with more investigation and comparisons across measures. It is depicted in Figure 6.

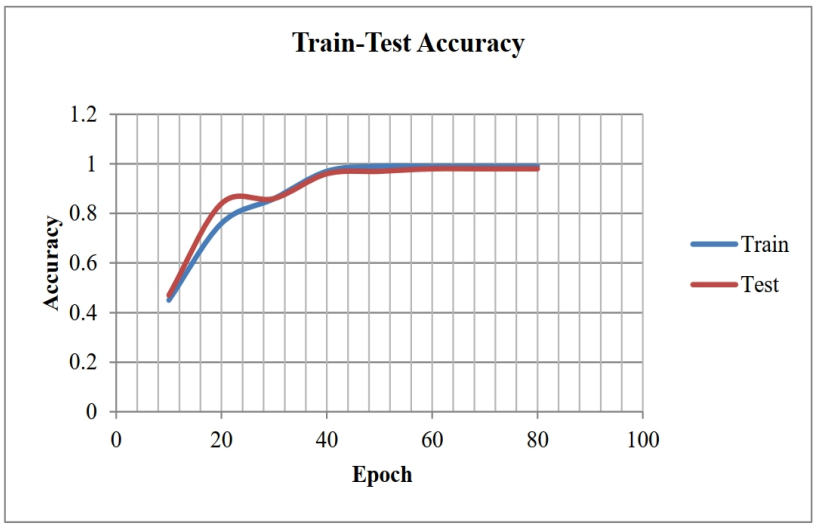

Figure 7: Train-Test Accuracy.

Figure 7 represents the training and testing accurateness. High train accuracy suggests that the model has successfully learned the features and patterns in the training data, while comparable high test accuracy signifies that the model can generalize well to new instances. Discrepancies between train and test accuracy can indicate potential issues such as overfitting, where the model memorizes the training data but fails to generalize, or underfitting, where the model inadequately captures the underlying patterns.

Figure 8 symbolizes the loss in testing and training. The difference or mistake between the model's predictions with the actual results on the training dataset is measured by the training loss. Its main goal is to minimize the

DOI: https://doi.org/10.54216/IJNS.230226

Received: October 24, 2023 Revised: November 30, 2023 Accepted: December 29, 2023

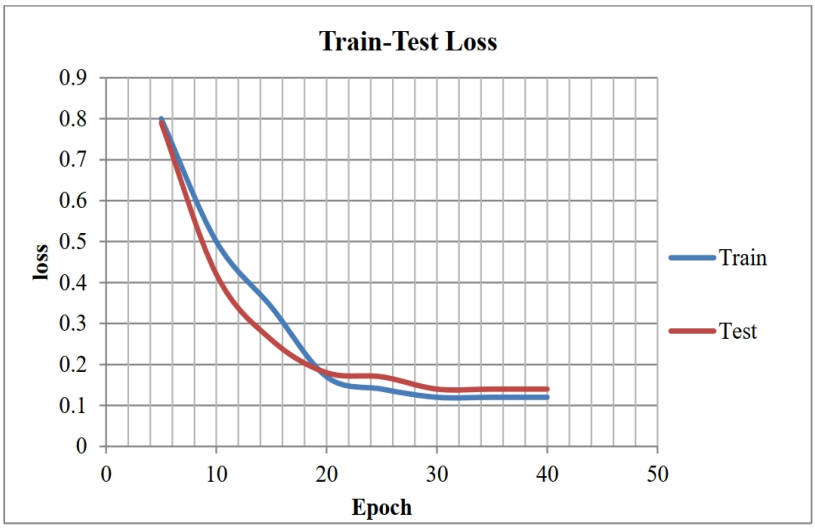

Figure 8: Training and Testing Loss.

discrepancy between expected and actual results by directing the model's parameter modifications throughout the training phase.

5.3 Discussion

The results obtained from the proposed HOG-SVM approach for skin cancer prediction demonstrate its remarkable effectiveness and superiority compared to existing methods. In Table 1, the HOG-SVM method exhibits an outstanding accuracy of 98.69%, outperforming LR, KNN, and GNB methods reported by Bechelli and Delhommelle in 2022, as well as CNN and Deep Belief Network methods presented by Tahir et al. in 2023. Further underscore the superiority of the proposed method, with values exceeding those of the comparative techniques. Additionally, when comparing datasets in Table 2, the ISIC 2020 dataset, used in the proposed method, outshines the ISIC 2017 and ISIC 2019 datasets in terms of accuracy, sensitivity, and specificity. Figures 5, 6, 7, and 8 provide visual representations of these comparative metrics, emphasizing the consistent and robust performance of the proposed HOG-SVM method. The higher accuracy and specificity, along with the visual representation of training and testing accuracy and loss, collectively validate the effectiveness of the proposed approach, showcasing its potential as a reliable tool for dermatological image analysis and skin cancer prediction.

6 Conclusion and Future Work

In conclusion, the Neutrosophic Fuzzy Logic-based SVM approach proposed in this study has demonstrated exceptional efficacy in enhancing skin cancer prediction. The comprehensive methodology, combining the power of neutrosophic sets, fuzzy logic, and support vector machines, has yielded superior results compared to existing methods, as evidenced by the significantly higher metrics. The utilization of the HOG-SVM architecture further strengthened the predictive capabilities of the model. The comparative analysis against LR, KNN, GNB, CNN, and Deep Belief Network methods, as well as the evaluation using different datasets, particularly the ISIC 2020 dataset, consistently highlighted the superior performance of the proposed approach. The visual representations of metrics and loss in Figures 5, 6, 7, and 8 provide a clear and compelling overview of the method's robustness and reliability. Future research avenues in this domain could explore the scalability and adaptability of the proposed Neutrosophic Fuzzy Logic-based SVM approach to larger and more diverse datasets. Investigating the model's performance with real-world clinical data and conducting prospective clinical trials would further validate its applicability in practical healthcare settings. Additionally, refinement and optimization of the model architecture, possibly incorporating deep learning techniques or ensemble methods,

DOI: https://doi.org/10.54216/IJNS.230226

Received: October 24, 2023 Revised: November 30, 2023 Accepted: December 29, 2023

could enhance predictive accuracy. Interpretability and explainability of the model's decisions are crucial in medical applications; hence, integrating explainable artificial intelligence (XAI) techniques can contribute to building trust and acceptance in clinical practice. Furthermore, collaborations with dermatologists and medical professionals can provide valuable insights for improving the model's clinical relevance. Overall, ongoing advancements in machine learning and medical imaging present exciting opportunities to continually enhance the accuracy and reliability of skin cancer prediction models for better patient outcomes.

Acknowledgment
The authors are thankful to the Deanship of Scientific Research at University of Bisha for supporting this work through the Fast-Track Research Support Program.

References

[1] A. Abdelhafeez, H. K. Mohamed, A. Maher, and N. A. Khalil, "A novel approach toward skin cancer classification through fused deep features and neutrosophic environment," *Frontiers in Public Health*, vol. 11, p. 1123581, 2023.

[2] S. Agrawal, R. Panda, P. K. Mishro, and A. Abraham, "A novel joint histogram equalization based image contrast enhancement," *Journal of King Saud University-Computer and Information Sciences*, vol. 34, no. 4, pp. 1172–1182, 2022.

[3] M. Ajmal, M. A. Khan, T. Akram, A. Alqahtani, M. Alhaisoni, A. Armghan, S. A. Althubiti, and F. Alenezi, "Bf2sknet: Best deep learning features fusion-assisted framework for multiclass skin lesion classification," *Neural Computing and Applications*, vol. 35, no. 30, pp. 22115–22131, 2023.

[4] J. R. Jebadass and P. Balasubramaniam, "Low light enhancement algorithm for color images using intuitionistic fuzzy sets with histogram equalization," *Multimedia Tools and Applications*, vol. 81, no. 6, pp. 8093–8106, 2022.

[5] M. Alqarni, A. H. Samak, S. S. Ismail, R. M. Abd El-Aziz, A. I. Taloba, *et al.*, "Utilizing a neutrosophic fuzzy logic system with ann for short-term estimation of solar energy," *International Journal of Neutrosophic Science*, vol. 20, no. 4, pp. 240–40, 2023.

[6] A. I. Taloba, M. Kanan, N. Omer, S. S. I. Ismail, and R. M. Abd El-Aziz, "Neutrosophic fuzzy neural network modelling and current-voltage analysis for forecasting post-surgery risks," *International Journal of Neutrosophic Science*, vol. 20, no. 4, pp. 232–239, 2023.

[7] T. Chaira, "Neutrosophic set based clustering approach for segmenting abnormal regions in mammogram images," *Soft Computing*, vol. 26, no. 19, pp. 10423–10433, 2022.

[8] S. K. Singh, V. Abolghasemi, and M. H. Anisi, "Skin cancer diagnosis based on neutrosophic features with a deep neural network," *Sensors*, vol. 22, no. 16, p. 6261, 2022.

[9] K. Bedair, N. Omer, A. A. H. Abdellatif, K. S. Nisar, S. R. Munjam, and A. I. Taloba, "Enhancing dorsalgia prediction using neutrosophic sets in a genetic algorithm-optimized hybrid cnn-lstm framework on spinal geometry parameters," *International Journal of Neutrosophic Science*, vol. 22, no. 3, pp. 99–118, 2023.

[10] A. H. Abdel Aty, A. A. H. Abdellatif, K. S. Nisar, S. R. Munjam, R. M. Abd El Aziz, and A. I. Taloba, "Utilizing neutrosophic logic in a hybrid cnn-gru framework for driver drowsiness level detection with dynamic spatio-temporal analysis based on eye aspect ratio," *International Journal of Neutrosophic Science*, vol. 22, no. 2, pp. 144–161, 2023.

[11] P. Jayaraman, N. Veeramani, R. Krishankumar, K. S. Ravichandran, F. Cavallaro, P. Rani, and A. Mardani, "Wavelet-based classification of enhanced melanoma skin lesions through deep neural architectures," *Information*, vol. 13, no. 12, p. 583, 2022.

[12] S. K. Singh, V. Abolghasemi, and M. H. Anisi, "Fuzzy logic with deep learning for detection of skin cancer," *Applied Sciences*, vol. 13, no. 15, p. 8927, 2023.

DOI: https://doi.org/10.54216/IJNS.230226

Received: October 24, 2023 Revised: November 30, 2023 Accepted: December 29, 2023

[13] A. S. Jaradat, R. E. Al Mamlook, N. Almakayeel, N. Alharbe, A. S. Almuflih, A. Nasayreh, H. Gharaibeh, M. Gharaibeh, A. Gharaibeh, and H. Bzizi, "Automated monkeypox skin lesion detection using deep learning and transfer learning techniques," *International Journal of Environmental Research and Public Health*, vol. 20, no. 5, p. 4422, 2023.

[14] K. A. Ogudo, R. Surendran, and O. I. Khalaf, "Optimal artificial intelligence based automated skin lesion detection and classification model.," *Computer Systems Science & Engineering*, vol. 44, no. 1, 2023.

[15] W. Gouda, N. U. Sama, G. Al-Waakid, M. Humayun, and N. Z. Jhanjhi, "Detection of skin cancer based on skin lesion images using deep learning," in *Healthcare*, vol. 10, p. 1183, MDPI, 2022.

[16] F. Afza, M. Sharif, M. A. Khan, U. Tariq, H.-S. Yong, and J. Cha, "Multiclass skin lesion classification using hybrid deep features selection and extreme learning machine," *Sensors*, vol. 22, no. 3, p. 799, 2022.

[17] N. Nigar, M. Umar, M. K. Shahzad, S. Islam, and D. Abalo, "A deep learning approach based on explainable artificial intelligence for skin lesion classification," *IEEE Access*, vol. 10, pp. 113715–113725, 2022.

[18] M. Q. Hatem, "Skin lesion classification system using a k-nearest neighbor algorithm," *Visual Computing for Industry, Biomedicine, and Art*, vol. 5, no. 1, pp. 1–10, 2022.

[19] R. M. Abd El-Aziz, A. I. Taloba, and F. A. Alghamdi, "Quantum computing optimization technique for iot platform using modified deep residual approach," *Alexandria Engineering Journal*, vol. 61, no. 12, pp. 12497–12509, 2022.

[20] "The isic 2020 challenge dataset." `https://challenge2020.isic-archive.com/`, Sept. 2023. Last accessed 05 Sep. 2023.

[21] M. Marghny, R. M. A. ElAziz, and A. I. Taloba, "Differential search algorithm-based parametric optimization of fuzzy generalized eigenvalue proximal support vector machine," *arXiv preprint arXiv:1501.00728*, 2015.

[22] A. Abozeid, R. Alanazi, A. Elhadad, A. I. Taloba, A. El-Aziz, M. Rasha, *et al.*, "A large-scale dataset and deep learning model for detecting and counting olive trees in satellite imagery," *Computational Intelligence and Neuroscience*, vol. 2022, 2022.

[23] A. Alsirhani, M. M. Alshahrani, A. Abukwaik, A. I. Taloba, R. M. Abd El-Aziz, and M. Salem, "A novel approach to predicting the stability of the smart grid utilizing mlp-elm technique," *Alexandria Engineering Journal*, vol. 74, pp. 495–508, 2023.

[24] N. Omer, A. H. Samak, A. I. Taloba, and R. M. Abd El-Aziz, "A novel optimized probabilistic neural network approach for intrusion detection and categorization," *Alexandria Engineering Journal*, vol. 72, pp. 351–361, 2023.

[25] A. I. Taloba, A. A. Sewisy, and S. S. Ismail, "Parameter tuning in decision tree based on genetic algorithm for text classification," *International Journal of Scientific Engineering and Research*, vol. 10, 2019.

[26] M. M. Abdelgwad, T. H. A. Soliman, and A. I. Taloba, "Arabic aspect sentiment polarity classification using bert," *Journal of Big Data*, vol. 9, no. 1, pp. 1–15, 2022.

[27] O. R. Shahin, R. M. Abd El-Aziz, and A. I. Taloba, "Detection and classification of covid-19 in ct-lungs screening using machine learning techniques," *Journal of Interdisciplinary Mathematics*, vol. 25, no. 3, pp. 791–813, 2022.

[28] S. Bechelli and J. Delhommelle, "Machine learning and deep learning algorithms for skin cancer classification from dermoscopic images," *Bioengineering*, vol. 9, no. 3, p. 97, 2022.

[29] M. Tahir, A. Naeem, H. Malik, J. Tanveer, R. A. Naqvi, and S.-W. Lee, "Dscc_net: Multi-classification deep learning models for diagnosing of skin cancer using dermoscopic images," *Cancers*, vol. 15, no. 7, p. 2179, 2023.

DOI: https://doi.org/10.54216/IJNS.230226

Received: October 24, 2023 Revised: November 30, 2023 Accepted: December 29, 2023